FREE VIBRATION ANALYSIS OF THIN, TENSIONED, HELICALLY WRAPPED WEBS USING MINDLIN-REISSNER FINITE ELEMENT METHOD

by

Ernesto Lopez[1], James Masters[2] and Sinan Müftü[1]
[1]Northeastern University
[2]CD-adapco
USA

ABSTRACT

Free vibration analysis of a thin tensioned web, wrapped around a reverser was studied. The effect of helix angle was considered. The eigen-problem was formed using finite elements and solved numerically. Design parameters such as tension, radius of cylinder, wrap angle, width of the web, lengths of non-wrapped web and helical wrap angle were studied. It was seen that the free edges cause a frequency clustering of the lateral-modes about the dominant longitudinal-mode. It was also seen that the effectiveness of the plate-shell junction to act as a stiff support depends on problem parameters. Eigenmodes with same mode-shape numbers are observed in symmetric and anti-symmetric fashion about the center of the plate, for configurations with equally long unwrapped sections. The results also showed that the first natural frequency is reduced at large helical angles for the parameters studied.

NOMENCLATURE

b	Width of the web
$\bar{D}$	Eigenmodes in matrix form
D_b	Bending rigidity $D_b = Eh^3/(12(1-\upsilon^2))$
D_t	In-plane stiffness $D_t = Eh/(1-\upsilon^2)$
E	Elastic modulus of the web, Pa
I	Second moment of area
h	Web thickness, m
L_1, L_2	Lengths of incoming/outgoing web, m
[K]	Global stiffness matrix
[M]	Global mass matrix
M_a	Bending moment (a = x, y)
p	Externally applied load
$R_w(x, y)$	Web radius of curvature
t	Time (sec)
T	Longitudinal external tension, N/m
w	Out-of-plane web deflection (m)
x,y	In-plane coordinate system
z	Transverse direction
β	Helix angle
$\lambda, {}^-\lambda, {}^+\lambda$	System eigenvalue, anti-symmetric, symmetric

ρ	Mass density of the web	v	Poisson's ratio of the web
θ	Wrap angle	∇^4	Biharmonic operator

INTRODUCTION

The manufacture of products in continuous web form benefits from models capable to predict their mechanical behavior under different conditions. This is necessary in order to suppress mechanical "failures" leading to product loss, and to improve the manufacturing speed. In a web handling application, such as photographic film or paper manufacturing, the running direction of a continuous web needs to change often. At certain process locations on the web-path, the web cannot be supported by rollers to change its direction, as contact could damage the product. *Air reversers* allow the web to float on a cushion of air, thereby protecting the web. An air reverser is a pressurized hollow drum with holes on the surface to provide the air cushion.

The behavior of a flexible web supported by an air reverser has been studied by Müftü and Cole [1]. They introduced a mathematical model of the interaction between the web and the air cushion formed by the air reverser. The governing equations of large web deflection were given, and coupled to a modified form of the Navier Stokes equations. It was seen that by wrapping the web around the cylinder, the web was stiffened by the added curvature. A parametric study of the web deflection was performed to identify problematic situations in the design of air reverser. Recently, the mechanics of a web helically wrapped around an air reverser has been investigated by Müftü [2]. The introduction of the helical angle reduced the shell stiffness, leading to higher web clearances.

The aspect ratio of the webs during manufacturing makes the process highly susceptible to transverse vibration. Raman *et al.* investigated the vibrations of paper webs [3]. Their work focused on an isotropic, linearly elastic, stationary and translating Kirchoff plate with a low stiffness-to-tension ratio. For stationary, uniformly tensioned plate with no fluid interaction, the cross span frequencies cluster to equivalent frequencies of a tensioned string. The frequency clustering leads to a dampening of vibrations in the center of a span and superposition of multiple modes at the free edges during excitation. At low and moderate transport speeds these frequency clusters remain distinct, but merge when translation is closer to the critical speed.

The coupling of spans in vibration of axially moving members was studied by Ulsoy [4]. The equations of motion were derived and solved for a closed-loop belt, tensioned over two pulleys while neglecting dampening effects. It was assumed that the belt had zero displacement at the pulleys. Energy transfer between the two spans was provided by a spring support at one of the pulleys. The beating phenomenon observed at low transport velocities disappeared at higher velocities or tension difference.

The present work investigates the behavior of the transverse vibrations of the tensioned web wrapped about a guide [2]. The model is represented by a plate-shell-plate configuration. It is assumed that the air cushion provided by the air reverser provides the gap in the shell area, but the fluid-structure coupling is not included in what follows. The stability of the system is studied. The FE method is used to investigate the influence of longitudinal tension (T), radius of the cylinder (R), wrap angle (θ), width of the web (b), lengths of incoming/outgoing webs (L_1, L_2) and helical wrap angle (β). The web transport is assumed to take place at moderately low speeds therefore, the gyroscopic acceleration components due to web transport are excluded from this study.

GOVERNING EQUATIONS

The formulation of this problem stems from the work by Müftü [2] where the differential equation, governing the mechanics of a web wrapped around a large cylindrical drum (Figure 1) under constant tension was derived.

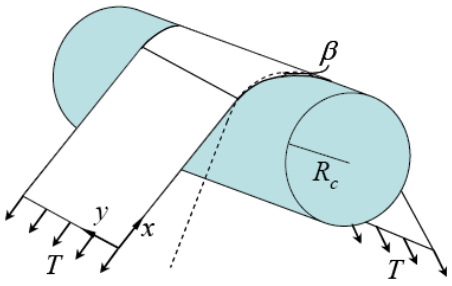

Figure 1 – The web and reverser with helical wrap.

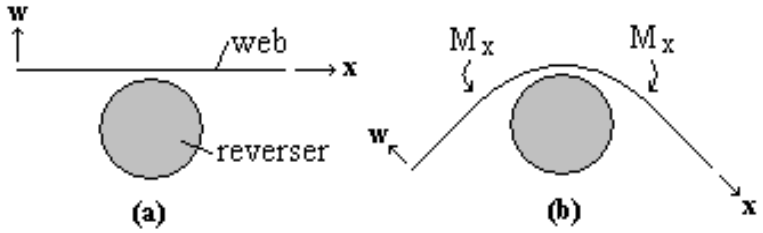

Figure 2 – (a) Drawing of web and reverser before application of bending moment, M_x. (b) Drawing of web and reverser after application of bending moment.

This process causes bending moments, M_x, to be "stored" in the wrapped section of the web. The webs attains an initial curvature, but the problem is formulated in the plane of the web (Figure 2). The tension is assumed to be constant T. A variant of the air reverser is the *turn-bar*, where the web is helically wrapped about the cylinder at an angle (β), (Figure 1). The turn-bar allows the web to change direction by an angle 2β, allowing for more versatility in a manufacturing floor layout. The helical angle alters the mechanics of the web. Here the equilibrium of the helically wrapped web [2] is modified to include the dynamic effects as follows,

$$\rho w_{,tt} + D_b \nabla^4 w + D_t \left(\cos^4\beta + \nu \cos^2\beta \sin^2\beta\right) \frac{w}{R_w^2(x,y)} - T w_{,xx} = p - \frac{T\cos^2\beta}{R_w} \qquad \{1\}$$

where, subscripted comma represents partial differentiation. Notice, that when the helical angle (β) is zero the original web equation developed in [1] is recovered.

SOLUTION METHOD

A finite element solution was developed for the steady-state problem by Masters [5] using bilinear, quadrilateral, Mindlin elements. The eigenvalue problem to study the undamped, free vibration behavior of the web is defined as,

$$\left\{[K]-\lambda^2[M]\right\}\left\{\overline{D}\right\}=0 \qquad \{5\}$$

where, λ is the natural frequency and $\overline{D}$ are the associated eigenmodes, by using $w(x,y,t)=\left\{\overline{D}\right\}e^{\lambda t}$.

The geometry of the analyzed web section is shown in Figure 3. The web consists of two thin plates, lengths L_1 and L_2, joined by a shell of radius R and length $R\theta$. The web is simply supported on opposite edges x=0 and x=L and free at the remaining two edges.

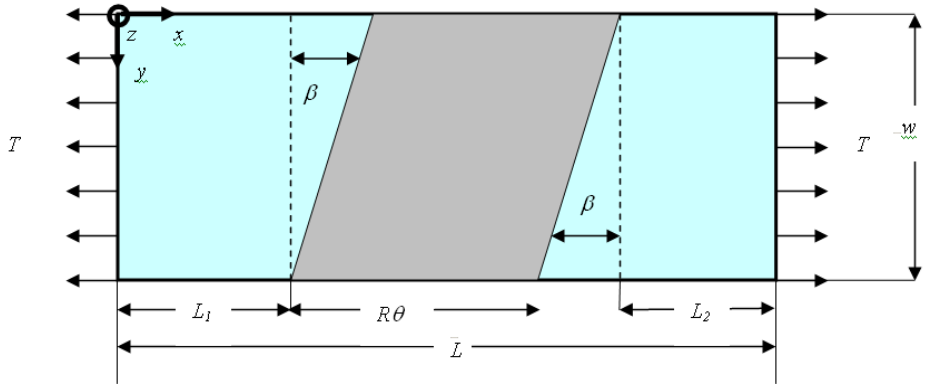

Figure 3 – Geometry of tensioned web under study. Gray area highlights the shell area. Simply supported at two opposite edges $x=0,L$.

In order to examine the effect of the mesh size on the solution, a study was conducted. The free vibrational response of a tensioned, cylindrically wrapped tape by Sundaram and Benson [6] was used to verify the natural frequencies and eigenmodes for both plate and shell solutions. This showed that the rate at which the error of the FE predictions grows depends on the eigenmodes of the frequencies. As the *m*-mode (*x*-direction or longitudinal mode) is held constant and *n*-mode (*y*-direction or lateral mode) increases, the rate at which the error grows increases. Due to the presence of the free boundaries, more *n*-modes are present as compared to the *m*-modes. This calls for a denser mesh in the *y*-direction. From this study, we decided a mesh of at least 21 nodes in the *x*-direction and 101 nodes in the *y*-direction for each section of plate or shell.

To test the ability of the model to predict plate-shell interaction, comparison was made with a tensioned-beam partially supported by an elastic foundation, shown Figure 4. The elastic foundation provided the added stiffness due to curvature, with the stiffness parameter defined as $k=Ehw/R^2$ from Equation {1}. In Appendix A, the governing equations and boundary conditions of the beam model are given. Comparison of the beam and FE models showed that the FE model predicts the longitudinal bending modes of the coupled plates-shell system with high accuracy. The simpler mechanical behavior

of the two-dimensional model will be utilized when discussing the results of the FE model.

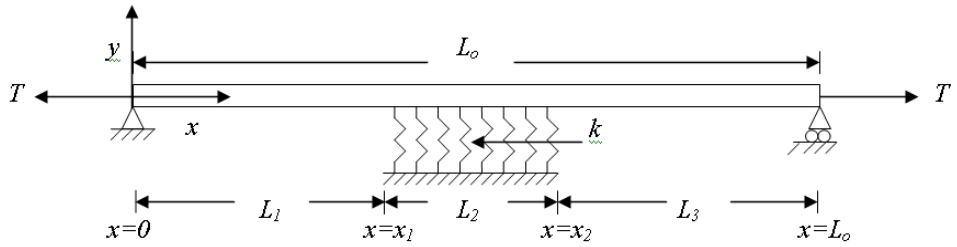

Figure 4 – Beam partially supported by an elastic foundation with simple support ends.

RESULTS AND DISCUSSION

In this section, the influence of design parameters on the vibration response of the tensioned web wrapped around a cylinder is discussed. Table 1 lists the parameters tested. We focus on the impact of each parameter on at least the first fifteen frequencies and mode shapes. The strain energy storage capability of the web depends on its physical parameters. In order to better understand the effect of the physical parameters, the critical frequencies will be examined along with the eigenmodes in this paper

R (m)	0.15
θ (deg)	30, 180
L_1 *(m)*	0.2, 1
L_2 *(m)*	0.2, 1
b (m)	0.25, 0.5
h (um)	25, 50, 100
T (N/m)	5,10, 50, 150
β (deg)	0,5,10,22.5,45

Table 1 – Design parameters varied for this study

Effect of Plate Length (L_1, L_2) and Wrap Angle (θ)

In plate vibrations, the web dimensions affect the plate's ability to resist transverse motion and its natural frequencies. An increase in the length of a plate or shell, causes a decrease in its effective stiffness and in its natural frequencies. Excitation of the plate and shell sections, for the cases studied here, remained largely independent due to the added curvature stiffness in the shell region. This difference in stiffness created an artificial spring support at the plate-shell boundary.

For plates of equal length lengths ($L_1 = L_2$), there exist eigenmodes which have the same mode numbers but are symmetric and anti-symmetric about the center of the plate. In Figure 5, shows two modes with identical mode numbers $m = 1$ and $n = 0$. The order of appearance of the symmetric/anti-symmetric modes, and the magnitude of their

frequencies depend on the effectiveness of the plate-shell junction to act as a stiff support. The shell section stiffness can be likened to a plate on an elastic foundation (Appendix A). The overall rigidity of the shell section is therefore a combination of its dimensions (length and width) and its radius of curvature.

In order to better illustrate the effectiveness of the plate-shell junction, Figure 6 highlights the "shell" region's modal response for different shell lengths, using the beam model. The length of the "shell" region is varied from L_2 = 1 m to 0.5 m. in Figures 6a and 6b, respectively. These figures show that the case with the longer "shell" region act stiffer, and plate-shell junction acts as stiff constraint. In Figure 6a, only a small length of the shell beyond the plate-shell junctions reacts, regardless of being a symmetric or anti-symmetric mode. As the length of the "shell" section decreases, the plate-shell boundary allows more deformation, as shown in Figure 6b. It should be noted that in Figure 6b anti-symmetric modes appear before symmetric modes, where $^{+}\lambda$ is slightly greater than $^{-}\lambda$.

In Figure 7 and Figure 8 the results of the FE model are given, where the first 15 m = 1 frequencies are shown for two wrap angles, $\theta = 30$ and 180 deg and two different web lengths $L_1 = L_2 = 1$, and 0.2 m, respectively. Both of these figures show that the larger wrap angle (180 deg) provides the stiffer plate-shell junction; and, the differences in frequencies of symmetric and anti-symmetric n-modes is negligible. As it was also noted in the beam model presented in Figure 6, by reducing the wrap angle, the antisymmetric n-modes ($^{-}\lambda$) appear first.

Notice in Figure 7, that while order in which modes appear may have shifted, the overall magnitudes of these first 15 modes did not vary. In Figure 8, the difference in stiffness between the plate and shell is reduced by shortening plate length. The frequency magnitude decreased for the first 15 modes when wrap angle was reduced, due to the lower difference in plate-shell stiffness.

The case involving plate sections of different lengths ($L_1 \neq L_2$) was also studied. While not shown here in this work, it was seen that the vibrational response of each plate or shell can be excited independently with only small excitation of the neighboring regions.

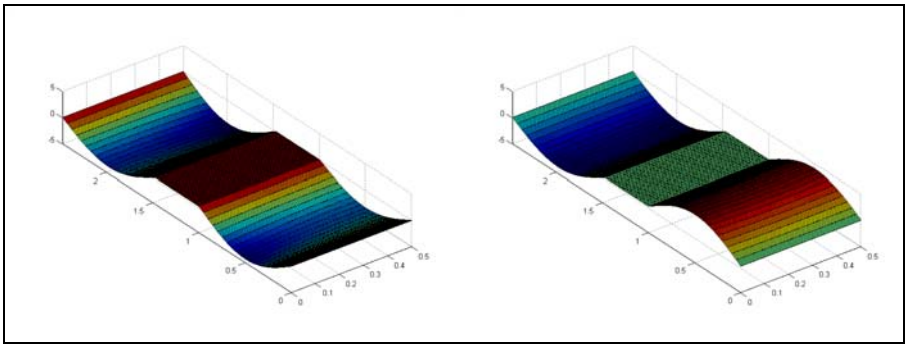

Figure 5 – Examples of symmetric (left) and anti-symmetric (right) modes. Shown here m = 1, n = 0, $+\lambda$ =103.03 *Rad/s*, $-\lambda$ =103.02 *Rad/s* , where L_1=L_2= 1.0 m , b=0.5, $h = 100$ μm, $R = 0.15$ m, $\theta = 180$ deg and T =150 N.

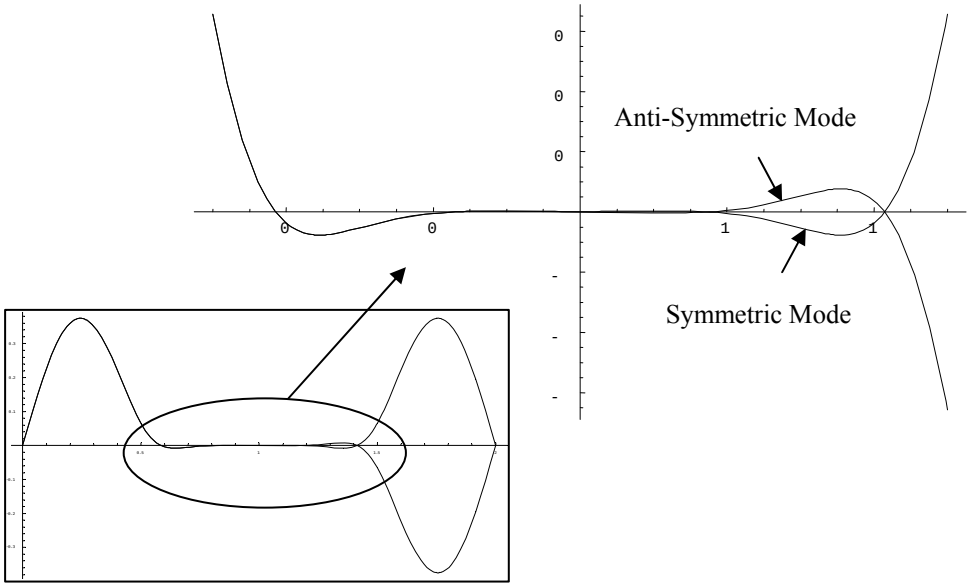

a) $L_2 = 1.0\ m,\ +\lambda = 238.42\ Rad/s,\ -\lambda = 238.42\ Rad/s$

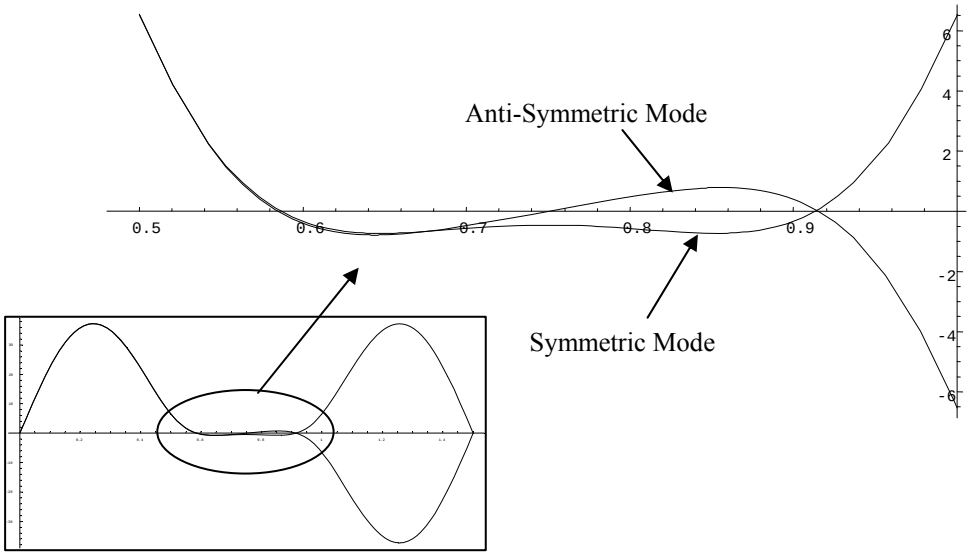

b) $L_2 = 0.5$ m, $+\lambda = 238.48$ Rad/s , $-\lambda = 238.37$ Rad/s

Figure 6 – Comparison of shell responses with varying stiffness during symmetric (+) and anti-symmetric (-) modes for beam model. Beam parameters are as follows $L_1 = L_3 = 0.5\ m$, $b = 0.01\ m$, $h = 0.01\ m$, $R = 1\ m$ and $T = 150\ N$. Shell length changed to vary stiffness.

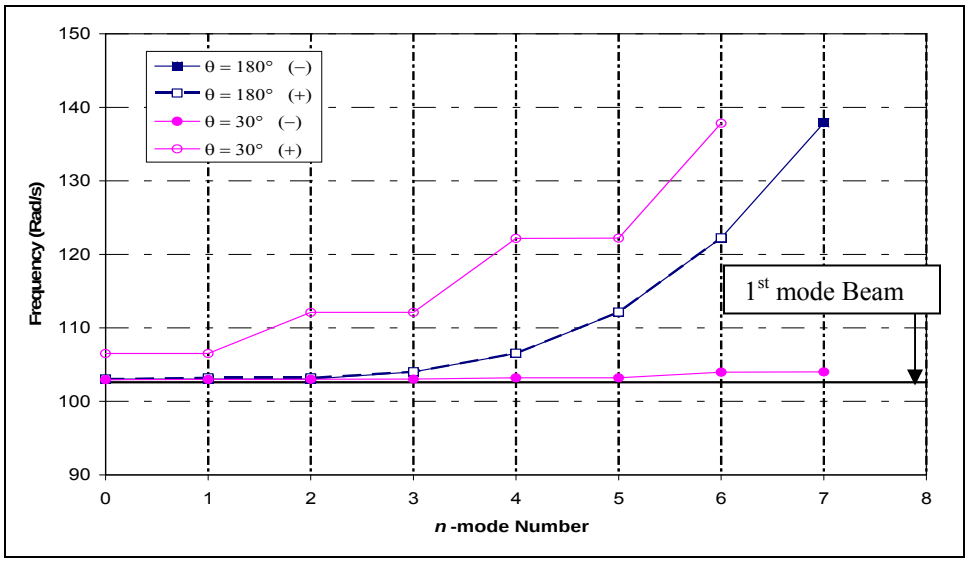

Figure 7 – First 15 m=1 frequencies for case where L_1=L_2= 1.0 m, b=0.5, h = *100 μm*, R = *0.15 m*, θ = *30, 180* deg and T =150 N.

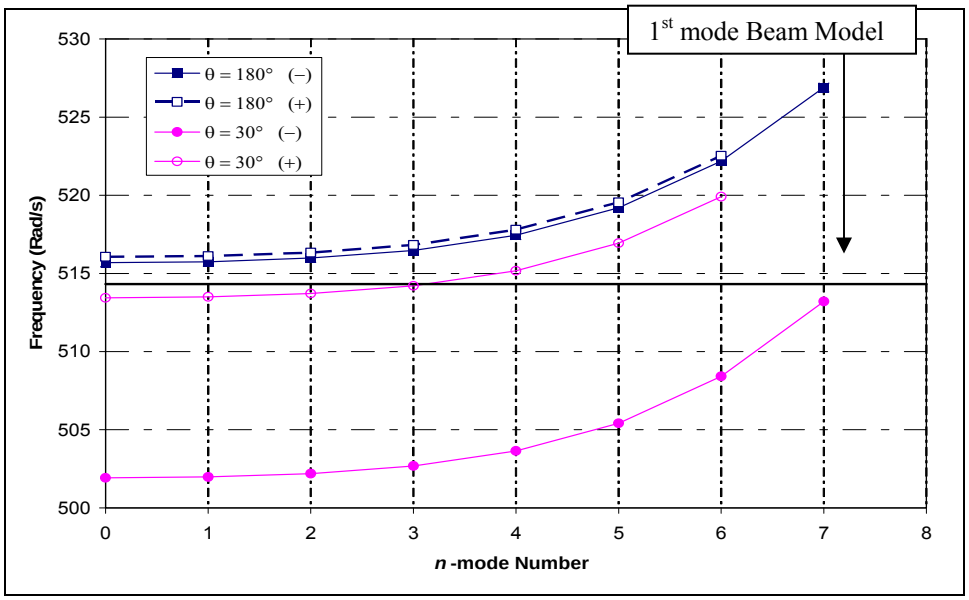

Figure 8 – First 15 m=1 frequencies for case where L_1=L_2= 0.2 m, b=0.5, h = *100 μm*, R = *0.15 m*, θ = *30, 180* deg and T =150 N.

Effect of Tension

It is expected that the web tension would have a strong effect on the magnitude of the natural frequencies as it provides a resistive (restoring force) for out-of-plane web deflection. This effectively stiffens the web. We find this stiffness increases the magnitude of the natural frequencies, and retards the appearance of higher m-modes. The magnitude of this effect varied depending on the other design parameters of the cases tested, but the increase in frequency applied to all cases. Frequency clustering, seen by Raman *et. al.*, is the grouping of *n*-modes around a dominant *m*-mode with frequencies equivalent to a tensioned string [3]. This clustering effect is increased for higher tension due to the suppression of higher *m*-modes. In Figure 9, the natural frequencies of the first six anti-symmetric (-) *n*-modes of $m = 1$ and the first $m = 2$ mode are shown for varying tensions. Due to the significant effect a small variation in tension has on mode shapes, a case with tension equal to 5 N has also been included. Notice that both the clustering effect for the first $m = 1$ modes and the natural frequencies increased for higher tensions. While all natural frequencies increased, the natural frequency for the first $m = 2$ mode increased at a much higher rate. In order to capture the detail in Figure 9, the magnitude of the natural frequency for the first $m = 2$ mode when $T = 150$ N ($-\lambda = 206.38$ *Rad/s*) was omitted, since it is twice that of the first $m = 1$ mode ($-\lambda = 103.02$ *Rad/s*).

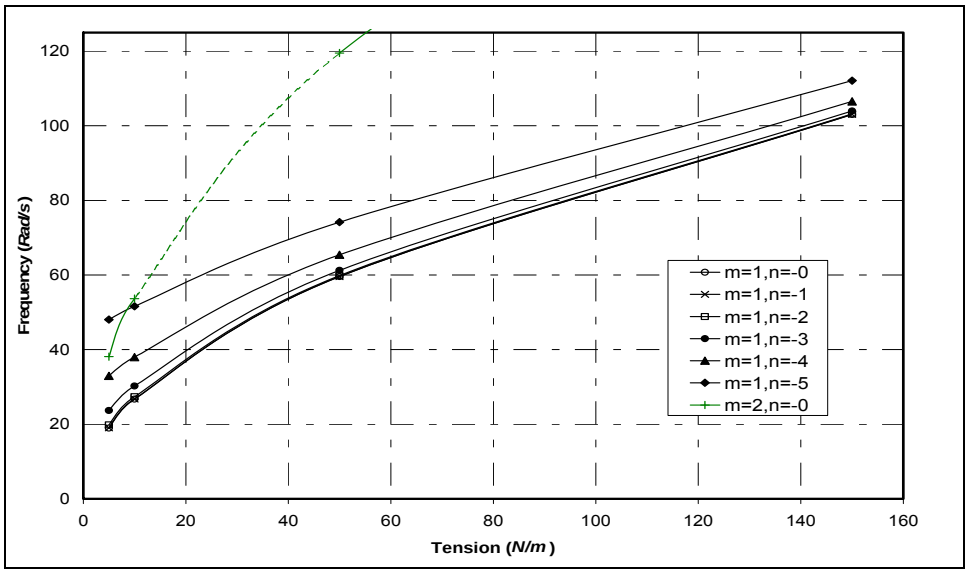

Figure 9 – Frequencies of first 6 anti-symmetric (-) *n*-modes of $m = 1$ and the first $m = 2$ mode, for case where $L_1 = L_2 = 1.0$ *m*, $b = 0.5$ *m*, $h = 100$ μm, $R = 0.15$ *m*, $\theta = 180$ deg and varying tensions.

Effect of Width (*b*) and Wrap Angle (θ)

It was stated before that the web dimensions influence its stiffness. It is expected that the narrower webs respond in a stiffer manner. Next the effect of the width of the web on the natural frequencies of the plate/shell system is investigated for $b = 0.25$ and 0.5 *m*. Figure 10 and Figure 11 show the change in frequency due to changing the web width, for different wrap angles $\theta = 180$ and 30 deg, respectively. While frequency clustering for the lower modes can be observed for both wide and narrow webs, in both of these

figures, the added stiffness in the *y*-direction reduces the clustering effect for the higher *n*-modes.

These figures also show the effects of the web width and wrap angle on the the ability of the plate/shell junction to act as a stiff constraint. By changing the width, the order in which the symmetric and anti-symmetric modes appear follows that of a plate with stiffer support. From this information and explanation of Figure 6, it is concluded that *decreasing the width of the web increases its constraining ability at the plate-shell junction*.

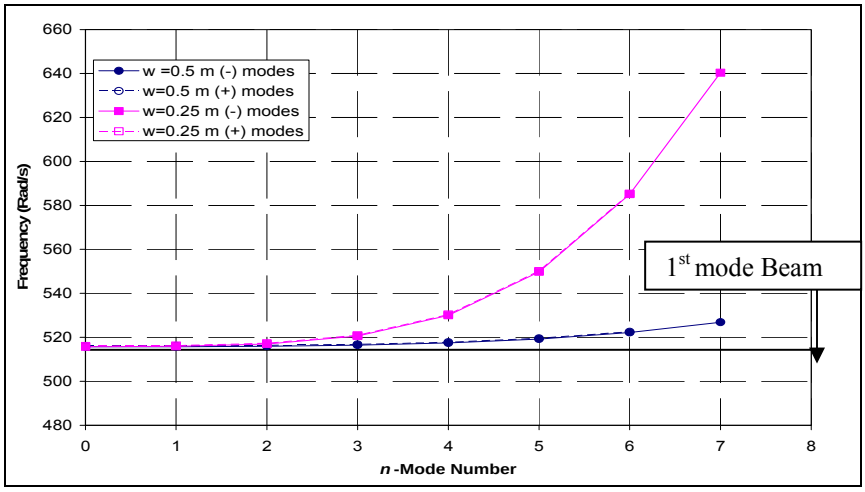

Figure 10 – First 15 *m*=1 frequencies for case where L_1=L_2= 0.2 *m*, *b*=0.25 and 0.5 *m*, *h = 100 um, R = 0.15 m, θ = 180* deg and *T* =150 *N*.

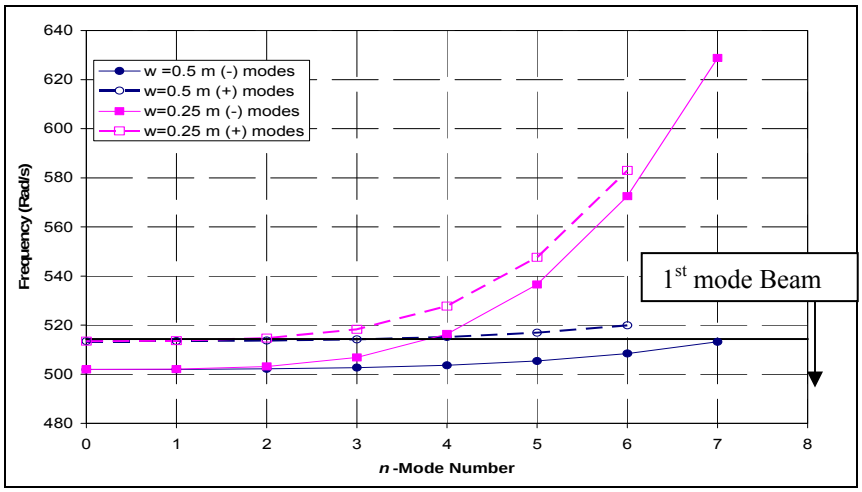

Figure 11 – First 15 *m*=1 frequencies for case where L_1=L_2= 0.2 *m*, *b*=0.25 and 0.5 *m*, *h = 100 μm, R = 0.15 m,* θ = 30 deg and *T* =150 *N*.

Effect of Helix Angle (β)

The implementation of a helix angle for a turn-bar system alters the dimensions of the incoming and exiting rectangular plates by elongation or contraction of the free edges to form a trapezoidal plate, as well as changing the shell stiffness [2]. The change in geometry affects the vibrational behavior described in previous sections. To examine the behavior of a turn-bar system, helix angles of $\beta = 0°, 5°, 10°, 22.5°$ and $45°$ were applied to a configuration with rectangular plates having initial dimensions of 1 m × 0.5 m. The helix angle was applied halfway across the width of the plate, so there to enable equal length changes at the opposite longitudinal edges, given as

$$\Delta x = \frac{b\tan(\beta)}{2}. \qquad \{26\}$$

As before, tension was varied for each model.

The previous sections have shown the effect of the stiffness of the shell region on the frequency and response of the plate sections. It was shown that increasing helix angle reduces the shell stiffness [2]. In order to provide a comparison for the effect of shell stiffness, the free vibrational response of a trapezoidal plate with simple-simple, free-free boundary conditions was solved using the ANSYS FEM package (ver.10.0, Canonsburg, Pennsylvania) for a small guide (R = 0.15 m). Figure 12 shows a comparison of our FE solution with the trapezoidal plate solution given by ANSYS. This shows that the shell stiffness still remains dominant despite the introduction of the large helical angle (β = *45),* providing a stiff support at the plate-shell junction.

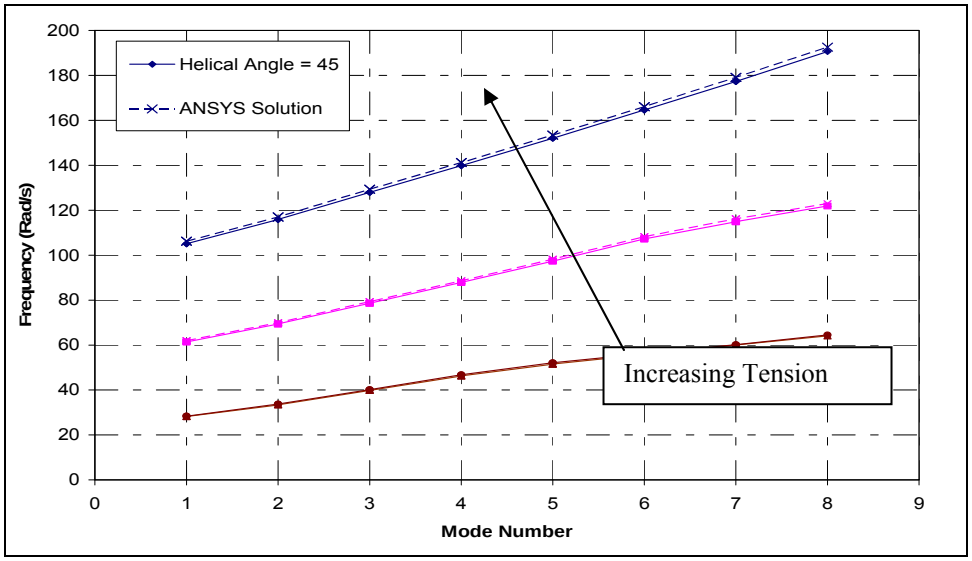

Figure 12 – First 8 frequencies for cases where L_1=L_2= 0.5 *m, b*=0.5, *h = 100 μm, R = 0.15 m, θ = 180* deg, varying *T =10, 50* and*150 N* with helical angle $\beta = 45°$.

This work also showed that applying the helical angle (about the midpoint of the width) stiffens half the plate while making the other half more compliant compared to the corresponding rectangular plate. Recall that the natural frequencies of the *n*-modes change faster than the *m*-modes due to the effect of the free-free lateral boundary

conditions. This variation of stiffness produces a set of "half" *n*-modes not present before in the rectangular modes, as shown in Figure 13a. These half *n*-modes appear during the transition of excitation of the more compliant half to the stiffer side for a given *m*-mode. Eventually, at higher natural frequencies the *n*-mode completely extends across the width of the plate resembling the rectangular plate modes and becoming a full n-mode, example shown in Figure 13b.

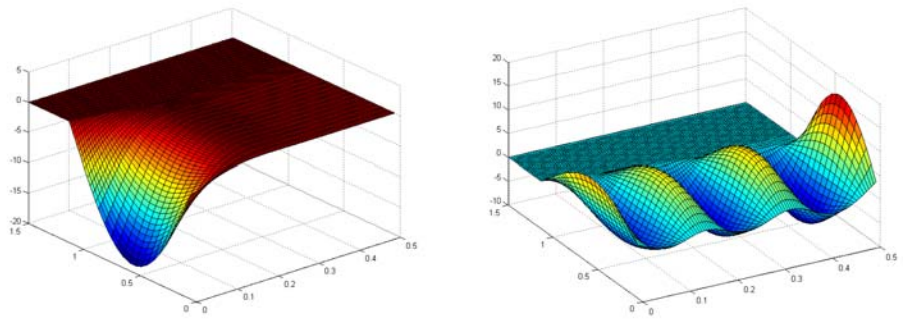

a) half *n*-mode, m=1 b) 6th *n*-mode, m=1

Figure 13 – Half and full *n*-mode comparison found for trapezoidal plate. Initial rectangular plate $L_1 = L_2 = 1$ *m*, $b = 0.5$ m, $h = 100$ μm, $R = 0.15$ m, $\theta = 180$ deg, and $\beta = 22.5$ deg, $T = 150$ N.

Comparing the natural frequencies of the helically wrapped webs and rectangular web ($\beta = 0$ deg), the effect of helical wrap could be further analyzed. Figure 14 shows the percentage of frequency change with respect to the $\beta = 0$ deg case as a function mode number with varying helix angles. Note that positive change corresponds to higher natural frequencies compared to a rectangular plate. The opposite is true for negative values. For the smaller helical angles, the natural frequencies increased. This indicates that the stiffer (shorter) side of the plate dominates the response. The difference in natural frequency increases for higher modes reaching a peak. The difference then decreases approaching zero. The peak change coincides with the disappearance of the half *n*-modes, as the whole plate is excited. As helical angle is increased, the longer, more compliant half of the trapezoidal plate is easier to excite, and the shell stiffness is lower, leading to lower natural frequencies. Again, the trend continues to positive difference peaking at the disappearance of the half n-modes. Figure 15 shows the frequency change due to varying tension for constant helical angle $\beta = 45$ deg. Increasing tension delays the *n*-mode at which the half *n*-modes disappear, and frequency change peaks. *Also note that the natural frequency is about 10% lower when the web is wrapped helically.*

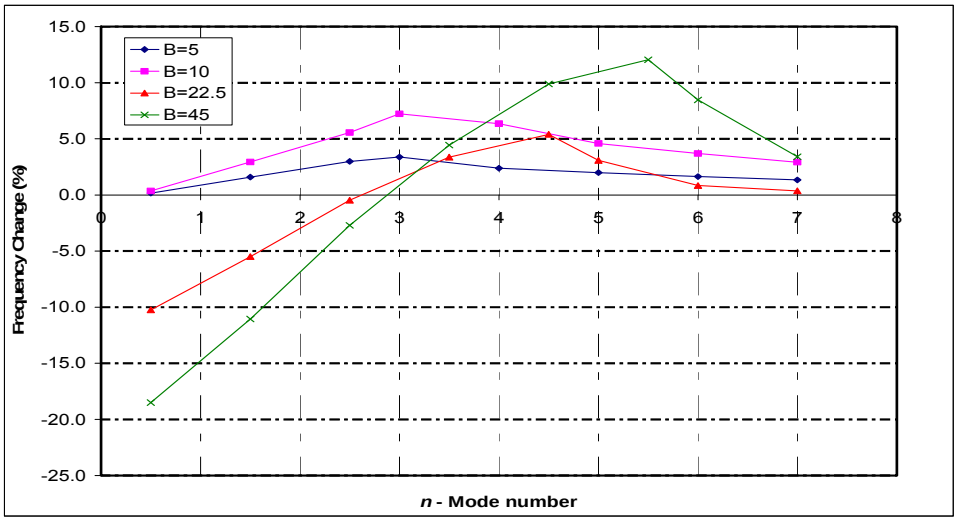

Figure 14 – Frequency change of (m=1,-n) modes as a function of helical angle. Initial rectangular plate $L_1 = L_2 = 1$ *m*, $b = 0.5$ *m*, $h = 100$ *μm*, $R = 0.15$ *m*, T=*150 N*, $\theta = 180$ deg. Helical angle varied β =*5, 10, 22.5, 45* deg.

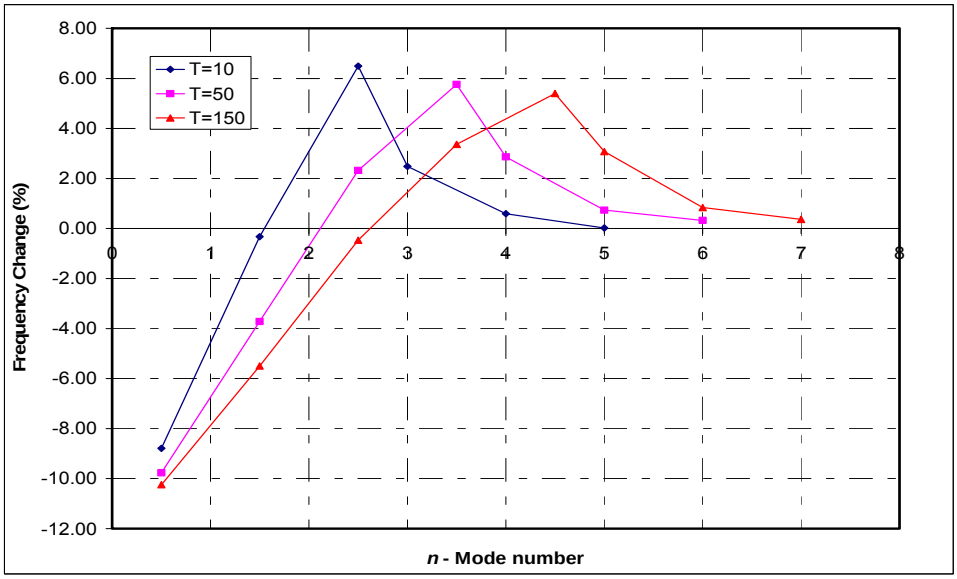

Figure 15 – Frequency change of (m=1,-n)modes as a function of tension. Initial rectangular plate $L_1 = L_2 = 1$ *m*, $b = 0.5$ *m*, $h = 100$ *μm*, $R = 0.15$ *m*, $\theta = 180$ *deg.* Helical angle $\beta = 45$ deg. Tension varied T =*10, 50 and 150 N.*

Effect of Radius (*R*)

In the previous sections, it has been shown that the difference in stiffness between the shell and plate section of the web stiffens the plate-shell junction, which in turn affects the coupling of the plates, and frequency magnitude. In previous cases the radius of the shell was kept constant at R = 0.15 m, and provided a much stiffer shell region when compared to the plate sections. Previously, the plate-shell junction was adjusted by varying the web dimensions, such as L_1, L_2, θ and b. The effect of changing the shell stiffness by using different guide radii is discussed using the beam model given in Appendix A.

The comparison is made between a beam partially supported by an elastic foundation, and a simply-supported beam of length $L_1 = L_3$ as defined in Figure 4. The elastic foundation stiffness is calculated as $k=Ehw/R^2$. The results are reported in relative change of frequencies. The change in the first natural frequency is shown in Figure 16 and Figure 17 for $L_1 = L_3 = 1$ and 0.2 m, respectively. These figures show that increasing the radius, weakens the shell region, and the effectiveness of plate-shell junction to act as a stiff support; leading to lower eigenvalues.

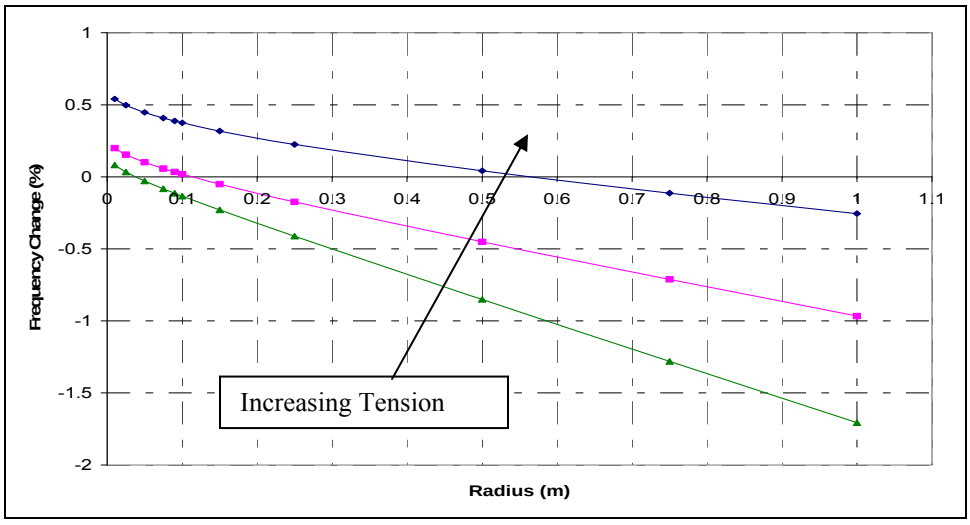

Figure 16 – Percent change in the first natural frequency of the two-dimensional tensioned beam partially supported by an elastic foundation compared to with that simply-supported tensioned-beam. $L_1 = L_3 = 1$ m, $b = 0.5$ m, $h = 100$ μm, $\theta = 180$ deg. Tension varied $T = 10, 50$ and 150 N. Radius varied $R = 0.15, 0.25, 0.5, 0.75, 1, 2$ and 5 m.

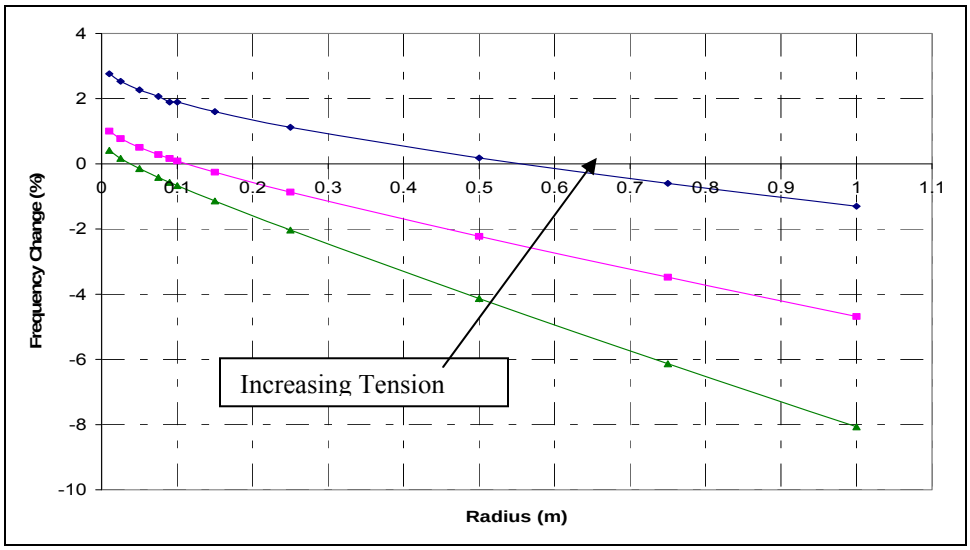

Figure 17 – Percent change in the first natural frequency of the two-dimensional tensioned beam partially supported by an elastic foundation compared to that with simply-supported tensioned-beam. $L_1 = L_3 = 0.2$ *m*, $b = 0.5$ *m*, $h = 100$ μ*m*, $\theta = 180$ deg. Tension varied $T = 10$, *50* and *150 N*. Radius varied $R = 0.15$, *0.25, 0.5, 0.75, 1, 2* and *5 m*.

SUMMARY

In this work, the free vibration analysis of a thin tensioned web wrapped around a reverser providing non-contact support analysis was performed. The eigen-problem was formed using finite elements and solved numerically. Design parameters such as tension (T), radius of cylinder (R), wrap angle (θ), width of the web (b), lengths of non-wrapped web ($L1$, $L2$) and helical wrap angle (β) were studied.

It was seen that the free edges cause a frequency clustering of the lateral n-modes about the dominant longitudinal m-mode, as also described by Raman *et al.* [3]. It was also seen that the effectiveness of the plate-shell junction to act as a stiff support depends on problem parameters. The results of this work can be summarized as follows:

- Plate Length (L_1, L_2) and Wrap Angle (θ): modify the effectiveness of the plate-shell junction as a stiff support. When $L_1 = L_2$, eigenmodes with same mode-shape numbers are observed in symmetric and anti-symmetric fashion about the center of the plate. Changes in plate-shell junction stiffness affect the appearance of symmetric and anti-symmetric modes and magnitude of the natural frequencies.
- Tension: has a strong effect on the magnitude of the natural frequencies, as it provides a resistive (restoring) force for out-of-plane web deflection. Higher tension suppresses the appearance of higher m-modes and causes increased frequency clustering.
- Web Width (b): The plate-shell junction acts as a stiffer support for smaller width. Reduced frequency clustering was observed for narrower webs.

- Helix Angle (β): Increasing the helix angle reduces the shell stiffness. While the shell stiffness is still dominant, the effective stiffness of the plate region is also modified, due to modified lengths of the free edges. Vibration modes, termed "half" n-modes, which are clustered near the longer edge are observed on the plate sections. The first natural frequency is reduced at large helical angles.
- Radius (R): The effectiveness of modeling the plate-shell junction as a stiff support improves for smaller guide radii.

REFERENCES

1. Müftü, S., Cole, K.A., "The Fluid/Structure Interaction of a Thin Flexible Cylindrical Web Supported by an Air Cushion," Journal of Fluids and Structures, Vol. 13, 1999, pp. 681-708.
2. Müftü, S., 2006, "Mechanics of a Thin, Tensioned-Shell, Wrapped Helically Around a Turn-Bar," Journal of Fluids and Structures, in print, 2007.
3. Raman, A., Wolf, K. Hagedorn, P. "Observations on the Vibrations of Paper Webs", Proc. of IWEB, Okalahoma State University, 2001.
4. Ulsoy, A. 1986, "Coupling Between Spans in the Vibration of Axially Moving Materials," Journal of Vibration and Acoustics, Vol.108, 207-211.
5. Masters, J., *A FEA of Web Wrapped About a Cylinder Using Shell Theory*, MS Thesis, Northeastern Univ., 2004.
6. Sundaram, R., Benson, R., C., 1989, "Transient Tape Deflection: A Mathematical Model" *private communication*.

APPENDIX A

In order to verify the accuracy of the interaction of the plate-shell interfaces, we solve the dynamic response of a beam partially supported by an elastic foundation, shown in Figure 1.

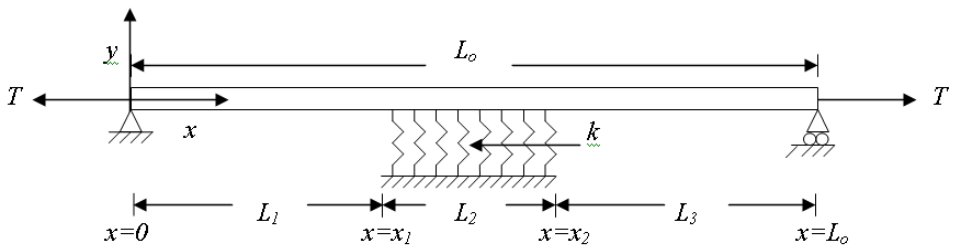

Figure 18 – Beam partially supported by an elastic foundation with simple support ends.

We begin by examining the governing equation for dynamics of a tensioned beam on an elastic foundation

$$\frac{\partial^2}{\partial x^2}\left(EI\frac{\partial^2 w}{\partial x^2}\right) - T\frac{\partial^2 w}{\partial x^2} + kw + m\frac{\partial^2 w}{\partial t^2} = 0 \qquad \{6\}$$

where E is the elastic modulus, I is the moment of inertia, T is the tension in N/m, m is the mass per unit length, k is the stiffness of the elastic foundation and w is the deflection

of the beam. To find natural frequencies of the equation we use separation of variables to represent the deflection as separate functions of time, $S(t)$ and displacement $W(x)$, such as

$$w(x,t) = W(x) \times S(t) . \qquad \{7\}$$

The differential characteristic equation is found by substituting equation {7} into equation {8} as;

$$W_{,xxxx} - \frac{T}{EI} W_{,xx} + \frac{k - m\lambda^2}{EI} W = 0 . \qquad \{8\}$$

This equation {8} has the following solution,

$$W(x) = C_1 e^{r_1 x} + C_2 e^{r_2 x} + C_3 e^{r_3 x} + C_4 e^{r_4 x} , \qquad \{9a\}$$

$$r_{1,2,3,4} = \pm \frac{1}{\sqrt{2}} \sqrt{\frac{T}{EI} \pm \sqrt{\left(\frac{T}{EI}\right)^2 + 4\frac{m\lambda^2 - k}{EI}}} . \qquad \{9b\}$$

We now represent the beam as three separate smaller beams, where for L_1 and L_3 have no elastic foundation present ($k = 0$) and L_2 has an elastic foundation with a stiffness parameter

$$k = \frac{E\,h\,b}{R^2} . \qquad \{14\}$$

The solution takes the form

$$W = \begin{cases} W_{L_1} & 0 \le x \le x_1 \\ W_{L_2} & x_1 \le x \le x_2 \\ W_{L_3} & x_2 \le x \le L_o \end{cases} \qquad \{15|$$

where,

$$W_{L_1}(x) = C_1 \sinh(r_1^*) + C_2 \cosh(r_2^*) + C_3 \sin(r_3^*) + C_4 \cos(r_4^*) \qquad \{16a\}$$

$$W_{L_2}(x) = C_5 e^{r_1 x} + C_6 e^{r_2 x} + C_7 e^{r_3 x} + C_8 e^{r_4 x} \qquad \{16b\}$$

$$W_{L_3}(x) = C_9 \sinh(r_9^*) + C_{10} \cosh(r_{10}^*) + C_{11} \sin(r_{11}^*) + C_{12} \cos(r_{12}^*) . \qquad \{16c\}$$

Note that for L_1 and L_3, $k = 0$ and the roots $r_{1,2,3,4}$ from {9b} are adjusted accordingly, denoted by (*).

To solve for the twelve constant coefficients we use the boundary and continuity conditions. Four boundary conditions come from the simple supports at the ends,

$$W_{L_1}(0) = 0 \qquad \{17a\}$$

$$W_{L_1,xx}(0) = 0 \qquad \{17b\}$$

$$W_{L_3}(L_o) = 0 \qquad \{17c\}$$

$$W_{L_3,xx}(L_o) = 0 \qquad \{17d\}$$

We can better accommodate boundary condition {17c} and {17d} by applying a different coordinate system on the third segment of the beam, L_3. The origin for the third segment is moved to simple support on this segment. Boundary conditions then reduce the deflection equations for L_1 and L_3 to

$$W_{L_1}(x) = C_1 \sinh(r_1^*) + C_3 \sin(r_3^*) \qquad \{18a\}$$

$$W_{L_3}(x) = C_9 \sinh(r_9^*) + C_{11} \sin(r_{11}^*) \qquad \{18b\}$$

The other eight boundary conditions come from the requirement that deflection, slope, shear and moment at junctions x_1 and x_2 are equal. Expressed in terms of deflection, these give continuous

$$W_{L_1}(x_1) = W_{L_2}(x_2) \qquad \{19a\}$$

$$W_{L_1,x}(x_1) = W_{L_2,x}(x_2) \qquad \{19b\}$$

$$W_{L_1,xx}(x_1) = W_{L_2,xx}(x_2) \qquad \{19c\}$$

$$W_{L_1,xxx}(x_1) = W_{L_2,xxx}(x_2) \qquad \{19d\}$$

$$W_{L_2}(x_2) = W_{L_3}(x_3) \qquad \{19e\}$$

$$W_{L_2,x}(x_2) = W_{L_3,x}(x_3) \qquad \{19f\}$$

$$W_{L_2,xx}(x_2) = W_{L_3,xx}(x_3) \quad \{19g\}$$

$$W_{L_2,xxx}(x_2) = W_{L_3,xxx}(x_3)\,. \quad \{19h\}$$

These eight boundary conditions lead to a set of eight homogenous equations which can represented in matrix form

$$[B]_{8x8}\{C\}_{8x8} = 0\,. \quad \{20\}$$

where, $\{C\}$ contains the vector of unknown coefficients. A non-trivial solution is only possible when

$$\mathrm{Det}[B] = 0\,. \quad \{21\}$$

Defining all parameters of the problem (i.e. *k, T, E,* etc.) the determinant is solely a function of frequencies (λ). Frequencies (λ) which satisfy equation {18} are the fundamental or natural frequencies. To plot eigenmodes, we input the natural frequency in Equation {20} and solve for the 8 coefficients in terms of one coefficient. We can then plot each individual section of the beam and normalize the eigenmode.

Free Vibration Analysis of Thin, Tensioned, Cylindrically Wrapped Webs Using Mindlin-Reissner Finite Element Method	**E. Lopez[1], J. Masters[2] & S. Müftü[1]**, [1]Northeastern University, [2]CD-adapco, USA

Name & Affiliation	**Question**
Herong Lei, Eastman Kodak	It appears that air is not modeled in the equation you are trying to resolve. You did mention that the tension changes the frequency?
Name & Affiliation	**Answer**
E. Lopez, Northeastern University	When you add resistance to the out-of-plane deformation by increasing your tension, a higher natural frequency results.
Name & Affiliation	**Question**
Herong Lei, Eastman Kodak	Are you talking about the vibration frequency of the web, up and down in that direction?
Name & Affiliation	**Answer**
E. Lopez, Northeastern University	Correct, these are transverse vibrations.
Name & Affiliation	**Question**
Herong Lei, Eastman Kodak	Do you have a rough estimate on what frequency would be associated with a tension level of 5 n/m?
Name & Affiliation	**Answer**
E. Lopez, Northeastern University	At 5 n/m of tension the frequency was 22 radian/second.